Chapter 4

Chiral Perturbation Theory in QCD

As it was mentioned in chapter 2, the low energy level of QCD cannot be treated with perturbation theory, but one can use lattice simulations. The analytic approach to this regime is the *Chiral Perturbation Theory*, which is an effective field theory. The Lagrangian of the effective theory is built by adding all the terms that are consistent with the symmetries of the underlying theory (QCD). This leads us to analize the chiral symmetry of the QCD Lagrangian.

4.1 QCD chiral symmetry

Since we are interested in low energy, we will work with the flavors whose masses satisfy $m_f \ll \Lambda_{\text{QCD}} \approx 300$ MeV. Therefore we only take into account the u and d quarks, with masses in the following range [1]

$$\begin{aligned} m_u &= 1.9 \text{ - } 2.65 \text{ MeV}, \\ m_d &= 4.5 \text{ - } 5.15 \text{ MeV}. \end{aligned} \tag{4.1}$$

Then, in Minkowski space-time, the Lagrangian is given by

$$\begin{aligned} \mathcal{L} &= \sum_{f=u,d} (\overline{q}_f i\gamma^\mu D_\mu q_f - m_f \overline{q}_f q_f) - \frac{1}{4} G^a_{\mu\nu} G_a^{\mu\nu}, \\ D_\mu &= (\partial_\mu + igA_\mu), \;\; G^a_{\mu\nu} = \partial_\mu A^a_\nu - \partial_\nu A^a_\mu + ig[A^a_\mu, A^a_\nu], \end{aligned} \tag{4.2}$$

where q_f and $\overline{q}_f$ are independent Grassmann fields associated to the flavor f and $A^a_\mu(x)$ are real valued fields related to the gauge field by $A_\mu(x) = \sum_{a=1}^{8} A^a_\mu(x) T_a$, where T_a are the basis elements of the traceless Hermitian 3×3 matrices. This implies that the gauge field is a matrix as well. The Lagrangian is constructed in the same way we did in section 2.3, so it is invariant under gauge transformations of SU(3). We are interested in analyzing the chiral symmetry, therefore we apply the chiral operators

$$P_R = \frac{1}{2}(\mathbb{I} + \gamma_5), \;\; P_L = \frac{1}{2}(\mathbb{I} - \gamma_5) \tag{4.3}$$

to the quark fields in order to obtain the right-handed and left-handed fields

$$q_{R_f} = P_R q_f, \;\; q_{L_f} = P_L q_f, \;\; \overline{q}_{R_f} = \overline{q}_f P_L, \;\; \overline{q}_{L_f} = \overline{q}_f P_R. \tag{4.4}$$

By using $\{\gamma_5, \gamma^\mu\} = 0$ and the definition of the chiral operators one can prove the following properties

$$P_{L,R} = P^\dagger_{L,R}, \;\; P^2_{L,R} = P_{L,R}, \;\; P_R P_L = P_L P_R = 0, \;\; P_{R,L}\gamma^\mu = \gamma^\mu P_{L,R}. \tag{4.5}$$

This implies

$$\begin{aligned} q_f &= q_{R_f} + q_{L_f}, \\ \overline{q}_f &= \overline{q}_{R_f} + \overline{q}_{L_f}. \end{aligned} \tag{4.6}$$

With eqs. (4.5) and eqs. (4.6) the QCD Lagrangian takes the form

$$\mathcal{L} = \sum_{f=u,d} \left[\overline{q}_{L_f} i\gamma^\mu D_\mu q_{L_f} + \overline{q}_{R_f} i\gamma^\mu D_\mu q_{R_f} - m_f(\overline{q}_{R_f} q_{L_f} + \overline{q}_{L_f} q_{R_f}) \right] - \frac{1}{4} G^a_{\mu\nu} G^{\mu\nu}_a. \tag{4.7}$$

Now, we use global chiral transformations defined by

$$q_{R,L_f} \to q'_{R,L_f} = e^{i\alpha\gamma_5} q_{R,L_f}, \;\; \overline{q}_{R,L_f} \to \overline{q}'_{R,L_f} = \overline{q}_{R,L_f} e^{i\alpha\gamma_5}, \;\; \alpha \in \mathbb{R}. \tag{4.8}$$

The mass term is not invariant under this transformations, so for the moment we will take $m = 0$. On the other hand, since $\{\gamma^\mu, \gamma_5\} = 0$ it follows that $\gamma^\mu e^{i\alpha\gamma_5} = e^{-i\alpha\gamma_5}\gamma^\mu$. As a result the Lagrangian transforms as

$$\begin{aligned} \mathcal{L} &= \sum_{f=u,d} \left(\overline{q}_{L_f} i\gamma^\mu D_\mu q_{L_f} + \overline{q}_{R_f} i\gamma^\mu D_\mu q_{R_f} \right) - \frac{1}{4} G^a_{\mu\nu} G^{\mu\nu}_a \\ &= \sum_{f=u,d} \left(\overline{q}'_{L_f} i\gamma^\mu D_\mu q'_{L_f} + \overline{q}'_{R_f} i\gamma^\mu D_\mu q'_{R_f} \right) - \frac{1}{4} G^a_{\mu\nu} G^{\mu\nu}_a. \end{aligned}$$

Hence, $\mathcal{L}$ is invariant under the transformations of eq. (4.8) only when $m = 0$, for that reason this is called the chiral limit. If we write the quark fields as vectors

$$q_{R,L} = \begin{pmatrix} q_{R,L_u} \\ q_{R,L_d} \end{pmatrix}, \;\; \overline{q}_{R,L} = \begin{pmatrix} \overline{q}_{R,L_u} \\ \overline{q}_{R,L_d} \end{pmatrix}, \;\; q = \begin{pmatrix} q_u \\ q_d \end{pmatrix}, \;\; \overline{q} = \begin{pmatrix} \overline{q}_u \\ \overline{q}_d, \end{pmatrix}, \tag{4.9}$$

it can be seen that the Lagrangian has a global symmetry $\mathrm{U}(2)_L \otimes \mathrm{U}(2)_R$. An element of U(2) can be decomposed into an element of SU(2) multiplied by a phase factor. Thus, we have the following symmetry group for the massless Lagrangian

$$\mathrm{U}(2)_L \otimes \mathrm{U}(2)_R = \mathrm{SU}(2)_L \otimes \mathrm{SU}(2)_R \otimes \mathrm{U}(1)_B \otimes \mathrm{U}(1)_A. \tag{4.10}$$

$\mathrm{U}(1)_A$ is known as axial symmetry and is broken explicitly under quantization. $\mathrm{U}(1)_B$ is associated with the baryon number conservation. Meanwhile, $\mathrm{SU}(2)_L \otimes \mathrm{SU}(2)_R$ is the chiral symmetry group. The latter breaks spontaneously to SU(2); the order parameter of this broken symmetry is the chiral condensate $\langle 0|\, \overline{q}q \,|0\rangle$, so when it is different from zero the chiral symmetry is indeed spontaneously broken. Because of the Goldstone theorem, to this broken symmetry corresponds $2^2 - 1 = 3$ massless Nambu-Goldstone Bosons (NGB). If now we take into account the masses m_u and m_d, the symmetry is explicitly broken and the NGBs turn into light massive quasi NGBs, which can be related to the pion triplet π^+, π^-, π^0. See refs. [2, 3, 4] for further details.

4.2 Effective Lagrangian

In order to build the effective Lagrangian $\mathcal{L}_{\text{eff}}$, one uses the dynamic variables suitable for low-energy. For two quark flavors this means that one replaces the quark and gluon fields by pion fields: $\vec{\pi} = \{\pi_1(x), \pi_2(x), \pi_3(x)\}$. Now one introduces a field $U(x) \in \mathrm{SU}(2)$

$$U(x) = \exp\left(i \frac{\vec{\pi} \cdot \vec{\tau}}{F_\pi} \right), \;\; \vec{\tau} = (\sigma_1, \sigma_2, \sigma_3), \tag{4.11}$$

that changes under global transformations of $\mathrm{SU}(2)_L \otimes \mathrm{SU}(2)_R$ as

$$U(x) \to U'(x) = \Omega_R U(x) \Omega_L^{-1}, \;\; \Omega_R \in \mathrm{SU}(2)_R, \;\; \Omega_L \in \mathrm{SU}(2)_L. \tag{4.12}$$

F_π is known as the pion decay constant and makes the argument of the exponential dimensionless; σ are the Pauli matrices, which are the generators of SU(2). Thus, $U(x)$ is rewritten as

$$U(x) = \exp\left(i\frac{\phi(x)}{F_\pi}\right), \;\; \phi(x) = \begin{pmatrix} \pi^0 & \sqrt{2}\pi^+ \\ \sqrt{2}\pi^- & -\pi^0 \end{pmatrix},$$
$$\pi^0 = \pi_3, \;\; \pi^\pm = \frac{\pi_1 \mp i\pi_2}{\sqrt{2}}. \tag{4.13}$$

$\mathcal{L}_{\text{eff}}$ is constructed by using $U(x)$. It must have all the terms that present the symmetries of QCD. Each term is accompanied by a number denominated low energy constant (LEC), that has to be determined from the underlying theory. However, there are actually an infinite number of terms consistent with the symmetries. They can be organized in increasing powers of momentum, which is the same as increasing number of derivatives, so one can truncate them for $m_f \ll \Lambda_{\text{QCD}}$. For the massless case, the effective Lagrangian with the least number of derivatives that can be written is

$$\mathcal{L}_{\text{eff}} = \frac{F_\pi^2}{4}\mathrm{tr}\left(\partial_\mu U \partial^\mu U^\dagger\right). \tag{4.14}$$

The factor of 4 is because if one expands in powers of ϕ, the kinetic term $\frac{1}{2}\mathrm{tr}(\partial_\mu\phi\partial^\mu\phi)$ is obtained. Under the transformation of eq. (4.12) the Lagrangian is invariant

$$\mathcal{L}_{\text{eff}} = \frac{F_\pi^2}{4}\mathrm{tr}\left(\Omega_R\partial_\mu U\Omega_L^{-1}\Omega_L\partial^\mu U^\dagger\Omega_R^{-1}\right) = \frac{F_\pi^2}{4}\mathrm{tr}\left(\Omega_R^{-1}\Omega_R\partial_\mu U\partial^\mu U^\dagger\right) = \frac{F_\pi^2}{4}\mathrm{tr}\left(\partial_\mu U\partial^\mu U^\dagger\right), \tag{4.15}$$

we have used the property $\mathrm{tr}(AB) = \mathrm{tr}(BA)$.

If one introduces the masses m_u and m_d to the theory, a term that explicitly breaks the chiral symmetry is added

$$\mathcal{L}_{\text{s.b.}} = \frac{F_0^2 B_0}{2}\mathrm{tr}\left(MU^\dagger - UM\right), \;\; M = \begin{pmatrix} m_u & 0 \\ 0 & m_d \end{pmatrix}, \tag{4.16}$$

where s.b. stands for symmetry breaking and F_0 and B_0 are two LECs. Then, to leading order the massive effective Lagrangian reads

$$\mathcal{L}_{\text{eff}} = \frac{F_\pi^2}{4}\mathrm{tr}\left(\partial_\mu U\partial^\mu U^\dagger\right) + \frac{F_0^2 B_0}{2}\mathrm{tr}\left(MU^\dagger - UM\right). \tag{4.17}$$

For degenerate quark masses $m_u = m_d \equiv m$, the LECs satisfy the following relations [5]

$$F_\pi = F_0\left[1 + O(m)\right],$$
$$\langle 0|\,\bar{q}q\,|0\rangle = -2F_0^2 B_0\left[1 + O(m)\right],$$
$$m_\pi = \sqrt{2B_0 m}\left[1 + O(m)\right]. \tag{4.18}$$

In the chiral limit $F_\pi = F_0$.

The effective Lagrangian can be formulated in terms of a normalized field $\vec{S}(x) \in \mathrm{O}(4)$ as well, since there is a local isomorphism between O(4) and $\mathrm{SU}(2)_L \otimes \mathrm{SU}(2)_R$. The symmetry breaking pattern also occurs

$$\mathrm{O}(4) \to \mathrm{O}(3) \leftrightarrow \mathrm{SU}(2)_L \otimes \mathrm{SU}(2)_R \to \mathrm{SU}(2). \tag{4.19}$$

The $\mathcal{L}_{\text{eff}}$ with less number of derivatives reads

$$\mathcal{L}_{\text{eff}} = \frac{F_\pi^2}{2}\partial_\mu \vec{S}\cdot\partial_\mu\vec{S}. \tag{4.20}$$

Now, we introduce an external field $\vec{H}$ that explicitly breaks the symmetry by adding the term

$$\mathcal{L}_{\text{s.b.}} = -\Sigma\vec{H}\cdot\vec{S}, \tag{4.21}$$

where $\Sigma \equiv -\langle 0|\,\overline{q}q\,|0\rangle$. $\vec{H}$ plays the same role as the quark mass. This is known as the non-linear σ model [6].

4.3 Chiral Perturbation Theory regimes

From eq. (4.17) it can be seen that the leading order LECs are F_π, B_0 and F_0. These constants can be determined trough lattice simulations by measuring the chiral condensate, the pion and degenerate quark masses and fitting the functions in eqs. (4.18). Nevertheless, one cannot simulate an infinite volume, so three regimes with finite volume in Euclidean space $V = L^d$ (note that we are taking the Euclidean time extension to be equal to the spatial volume), with d the dimension, have been established. For each one of them, eqs. (4.18) can be different, but the LECs are the same. Let us briefly review the regimes:

- The first regime we discuss is the *p-regime*. It consists of a large volume compared to the correlation length: $L \gg \xi = m_\pi^{-1}$. In this regime the finite volume corrections are suppressed by a factor proportional to $\exp(-m_\pi L)$, so eqs. (4.18) are valid [5].
- If $L \lesssim \xi$ then we refer to the so-called *ϵ-regime* [7]. Here the finite volume corrections cannot be neglected. In this regime the chiral condensate has the following dependence on the LECs, m and the volume when $B_0 m L^2 \ll 1$

$$\langle 0|\,\overline{q}q\,|0\rangle = -2F_0^2B_0\left(\frac{I_1'(F_0^2B_0mV)}{I_1(F_0^2B_0mV)} - \frac{1}{F_0^2B_0mV}\right), \tag{4.22}$$

  where I_1 is the modified Bessel function of first kind of order one. When one takes the infinite volume limit, the chiral condensate yields $\langle 0|\,\overline{q}q\,|0\rangle = -2F_0^2B_0$, recovering the second line of eqs. (4.18). On the other hand, when $m \to 0$, eq. (4.22) yields (see ref. [8] for details)

$$\langle 0|\,\overline{q}q\,|0\rangle = -\frac{1}{2}F_0^4B_0^2mV. \tag{4.23}$$

  We can see that in the chiral limit $\langle 0|\,\overline{q}q\,|0\rangle$ vanishes. This is consistent with the fact that in finite volume there is no spontaneous symmetry breaking.
- Finally, the *δ-regime* is determined by a volume of size $V = L^3\times L_t$, where the spatial volume is small, but the Euclidean time extension is large, that is $L \lesssim \xi \ll L_t$.

The pion decay constant has already been calculated in the p-regime and the ϵ-regime with 3 flavors several times, giving a result of $F_\pi = 92.1(9)$ MeV [9, 10, 11, 12]. Meanwhile, the δ-regime is less explored; there F_π has been measured with two flavors obtaining $F_\pi = 78^{+14}_{-10}$ MeV [13].

This last regime is useful from a technical point of view, because the small volume reduces the computing time of the simulations. Besides, the fact that $L \lesssim \xi$ has different effects. First, in the chiral limit the pion mass does not become massless and instead there is a *residual mass* $m_\pi^R \neq 0$. Another consequence is that there is approximately only one dimension, that enables us to treat the system as a quasi one dimensional field theory, *i.e.* quantum mechanics [14]. Then, in the O(4) model, $\vec{S}(x)$ describes approximately a

particle moving in a unit sphere. One can express m_π^R as the energy gap of a quantum rotor, which is given by

$$E_j = \frac{j(j+N-2)}{2\Theta}, \tag{4.24}$$

where Θ is the moment of intertia and N stands for the O(N) group. The value of Θ was computed in ref. [15] for a general dimension d and N

$$\Theta = F_\pi^2 L^{d-1}\left[1 + \frac{N-2}{4\pi F_\pi^2 L^{d-2}}\left(2\frac{d-1}{d-2} + \cdots\right)\right]. \tag{4.25}$$

m_π^R is obtained by substituting $j = 1$ and $N = 4$ in eq. (4.24)

$$m_\pi^R = \frac{3}{2\Theta}. \tag{4.26}$$

In four dimensions we have

$$m_\pi^R = \frac{3}{2F_\pi^2 L^3(1+\Delta)}, \;\; \Delta = \frac{0.477\cdots}{(F_\pi L)^2} + \ldots, \;\; d = 4. \tag{4.27}$$

However, in two dimensions there is a divergence of the next-to-leading term, so instead we just consider the leading term, yielding

$$m_\pi^R \simeq \frac{3}{2F_\pi^2 L}, \;\; d = 2. \tag{4.28}$$

This dimension has not been considered in this context, because there are no NGBs [16]. Still, at finite fermion mass the lightest particles are similar to quasi NGBs and we will refer to them as pions. Note that when $d = 2$, F_π does not have units.

Several simulations of the two flavor Schwinger model were performed in the the δ-regime with the HMC algorithm. This allows to obtain m_π^R as a function of L, in order to revise eq. (4.28) and extract the value of F_π.

4.4 δ-regime results

To acquire results for the residual pion mass, one has to fix a value for the gauge coupling constant g. As in chapter 3, we will denote $\beta = 1/g^2$. Results for $\beta = 2, 3$ and 4 were obtained. In figure 4.1 (a), m_π is shown as a function of the degenerate quark mass m for $L = 6$, $L_t = 64$ and $\beta = 4$. We can see that close to the chiral limit, the value of m_π becomes very unstable, so one cannot simply measure m_π at $m = 0$. Instead one extrapolates the value to $m = 0$. However, that is easier to do with figure 4.1 (b), where m_π is plotted against $(m^2 g)^{1/3}$. A function of the form $y = \sqrt{a + bx^3}$, where $x = (m^2 g)^{1/3}$ and a and b are fit parameters, was fitted to extrapolate m_π^R. Many tries with functions of the form $y = \sqrt{a + bx^c}$ and $y = a + bx^c$ were performed. The best results were obtained by taking $c = 3$ in the former expression. We do not have an explanation for this behavior, but it works to infer m_π^R.

This same procedure was done for different L between 5 and 12 and $L_t = 64$. In figure 4.4 plots of m_π vs. $(m^2 g)^{1/3}$ are shown for $\beta = 4$, in figure 4.3 for $\beta = 3$ and in figure 4.2 for $\beta = 2$.

Finally, one plots m_π^R as a function of L and fits a function of the form $3/2LF_\pi^2$, as it is shown in figures 4.5, 4.6 and 4.7.

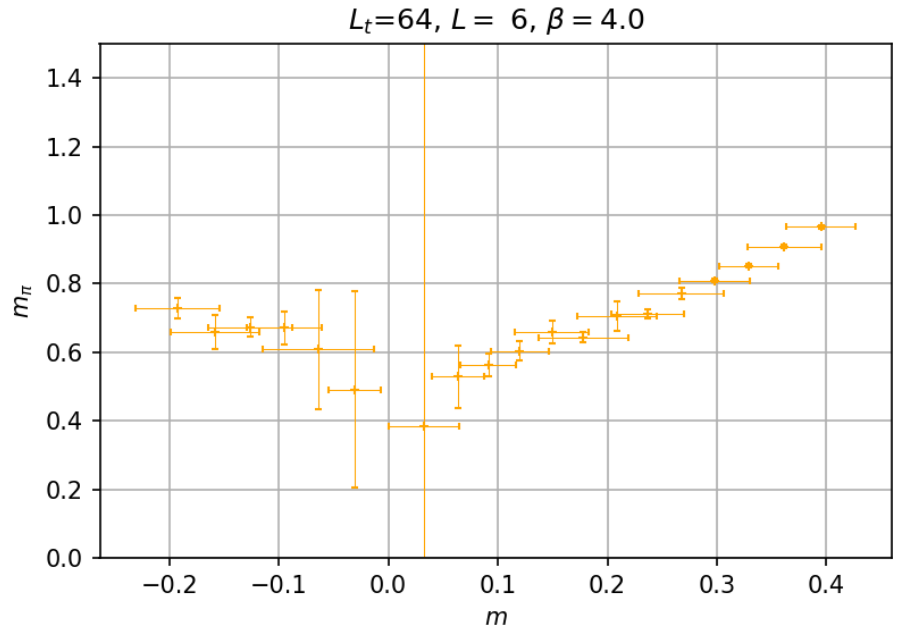

(a) m_π vs. m. It can be seen that near $m = 0$ the pion mass result is not trustable.

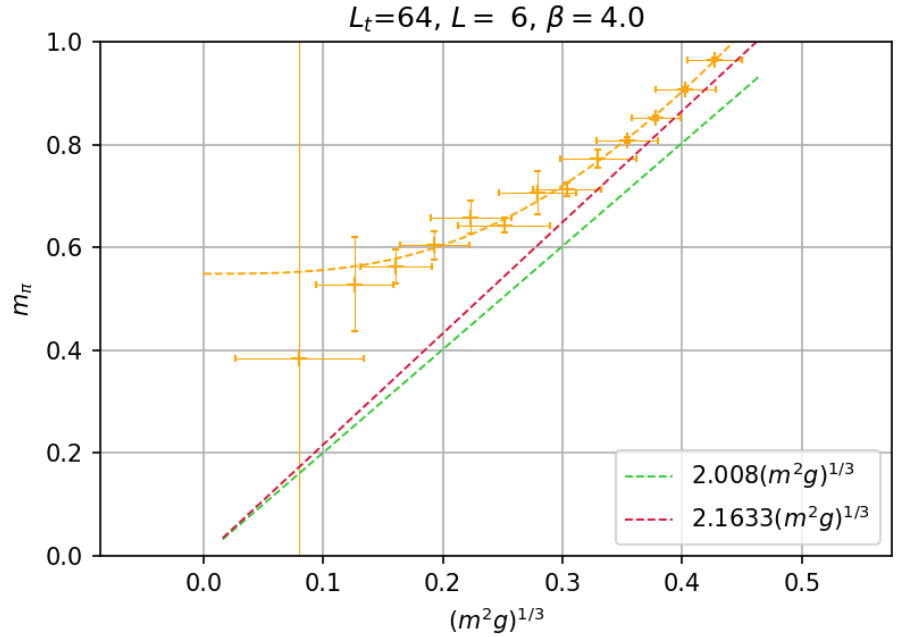

(b) m_π vs. $(m^2g)^{1/3}$. One can a function of the form $y = \sqrt{a + bm^2g}$ to obtain the value of the residual pion mass: $m_\pi^R = 0.5487(117)$. The predictions for m_π at finite temperature, mentioned in chapter 3, are shown as well.

Figure 4.1: Results of m_π and m. Note that there are also values for $m < 0$, they are unphysical. However, in the simulation both masses have to be measured through other parameter of the HMC algorithm, which allows negative fermion masses. In the lower plot only $m > 0$ was considerd. The errors were computed by using the *Jackknife method*.

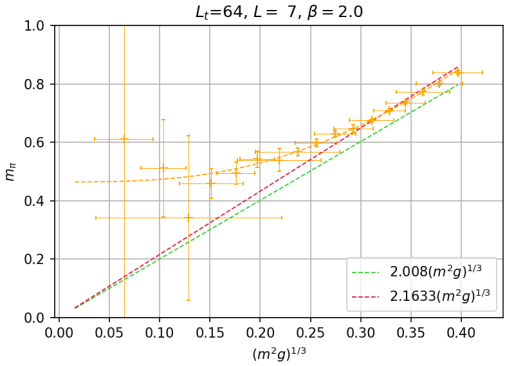

(a) m_π vs. $(m^2g)^{1/3}$ for $L = 7$. m_π =0.4645(72)

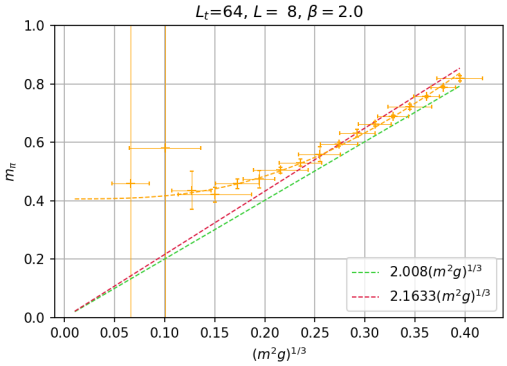

(b) m_π vs. $(m^2g)^{1/3}$ for $L = 8$. m_π =0.4063(45)

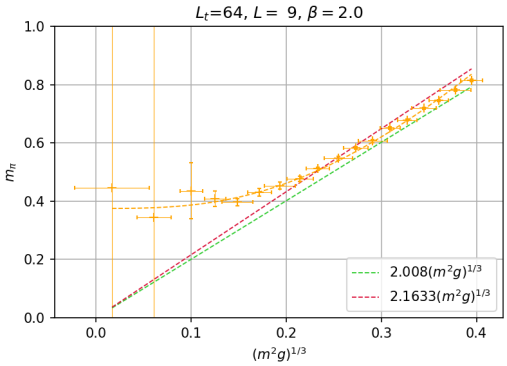

(c) m_π vs. $(m^2g)^{1/3}$ for $L = 9$. m_π =0.3749(47)

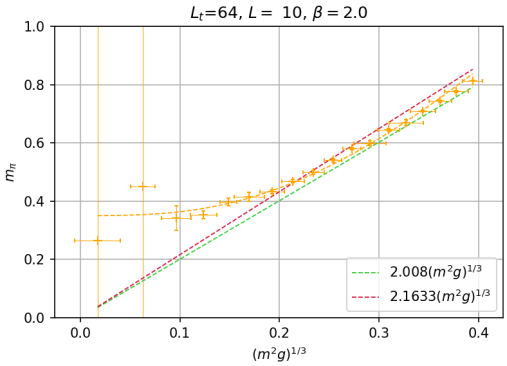

(d) m_π vs. $(m^2g)^{1/3}$ for $L = 10$. m_π =0.3505(58)

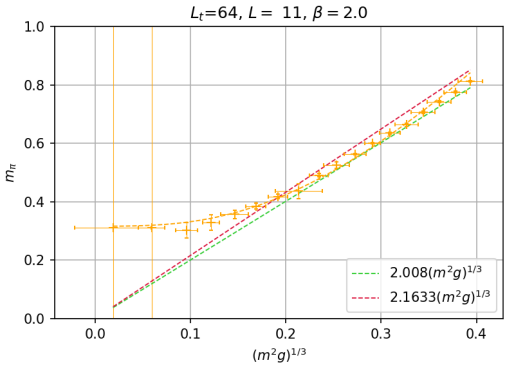

(e) m_π vs. $(m^2g)^{1/3}$ for $L = 11$. m_π =0.3163(59)

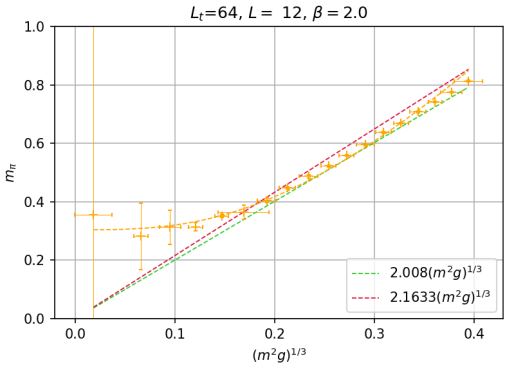

(f) m_π vs. $(m^2g)^{1/3}$ for $L = 12$. m_π =0.3040(51)

Figure 4.2: Results for $\beta = 2$. Each value of m_π and m was obtained by averaging 1,000 measurements of different configurations. Between each configuration used, 10 sweeps were performed. All the fits were made with gnuplot.

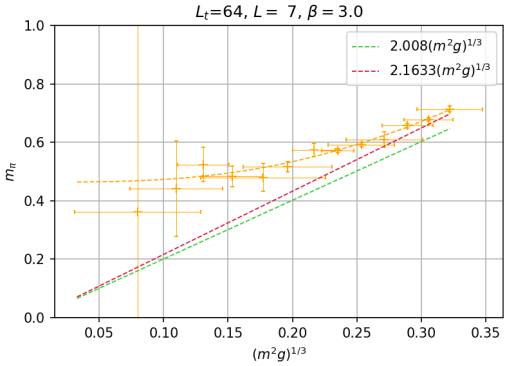

(a) m_π vs. $(m^2g)^{1/3}$ for $L = 7$. m_π =0.4639(103)

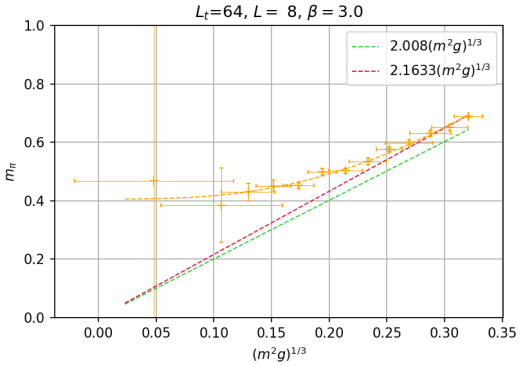

(b) m_π vs. $(m^2g)^{1/3}$ for $L = 8$. m_π =0.4057(58)

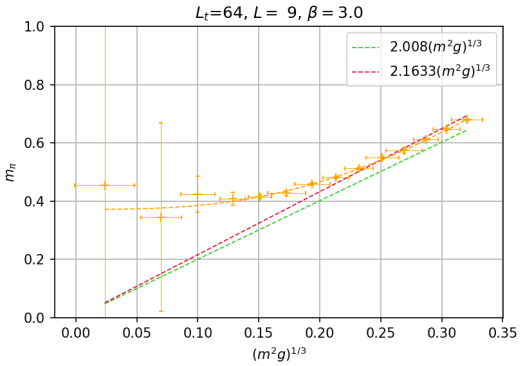

(c) m_π vs. $(m^2g)^{1/3}$ for $L = 9$. m_π =0.3722(29)

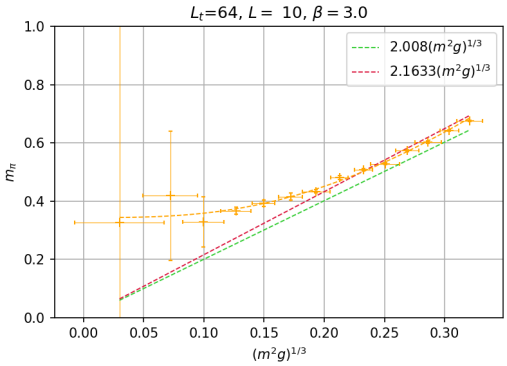

(d) m_π vs. $(m^2g)^{1/3}$ for $L = 10$. m_π =0.3437(42)

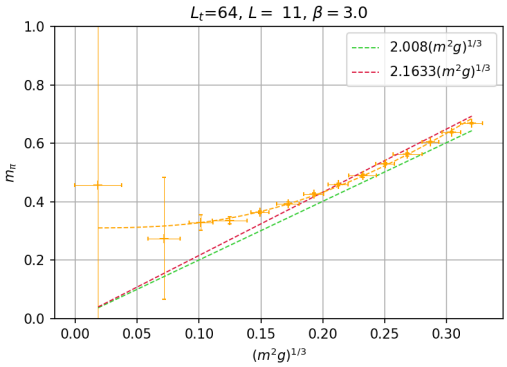

(e) m_π vs. $(m^2g)^{1/3}$ for $L = 11$. m_π =0.3104(30)

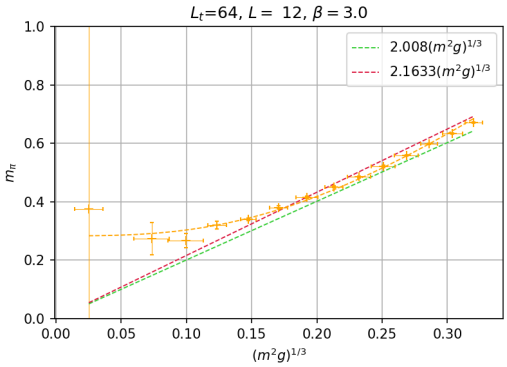

(f) m_π vs. $(m^2g)^{1/3}$ for $L = 12$. m_π =0.2832(51)

Figure 4.3: Results for $\beta = 3$. Each value of m_π^2 and m was obtained by averaging 1,000 measurements of different configurations. Between each configuration used, 10 sweeps were performed.

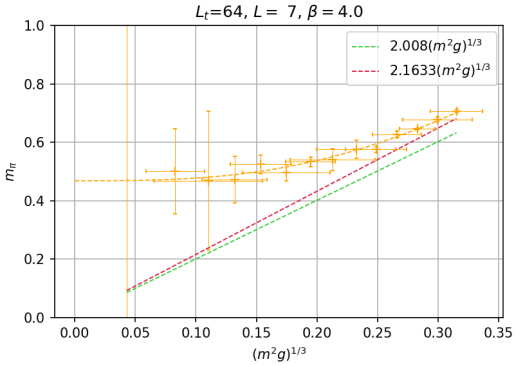

(a) m_π vs. $(m^2g)^{1/3}$ for $L = 7$. m_π =0.4684(75)

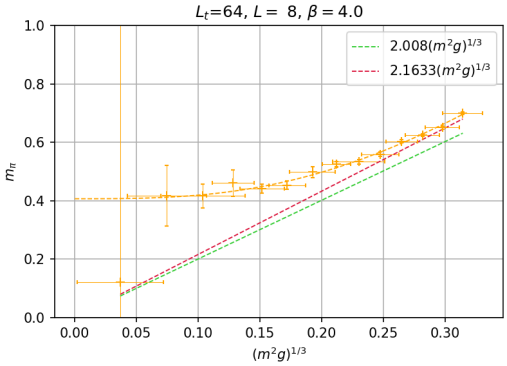

(b) m_π vs. $(m^2g)^{1/3}$ for $L = 8$. m_π =0.4068(63)

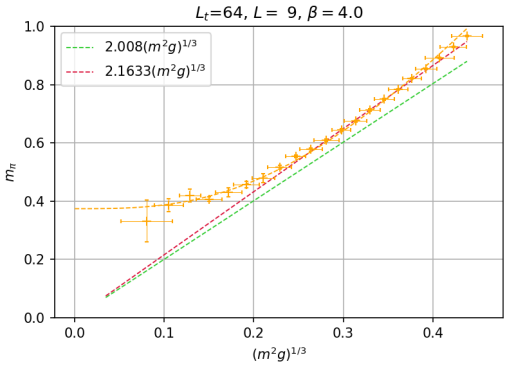

(c) m_π vs. $(m^2g)^{1/3}$ for $L = 9$. m_π =0.3741(40)

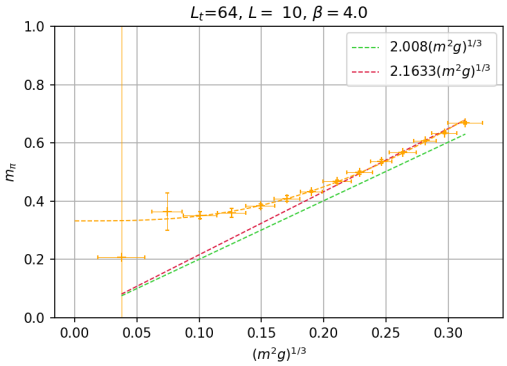

(d) m_π vs. $(m^2g)^{1/3}$ for $L = 10$. m_π =0.3323(22)

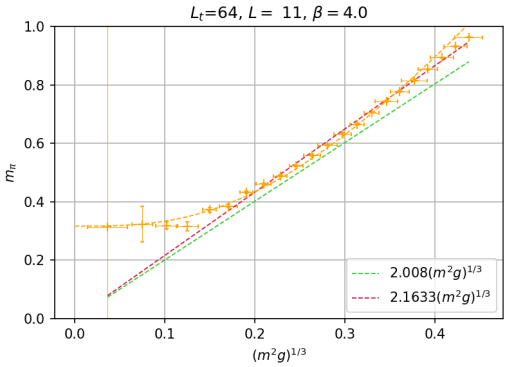

(e) m_π vs. $(m^2g)^{1/3}$ for $L = 11$. m_π =0.3167(54)

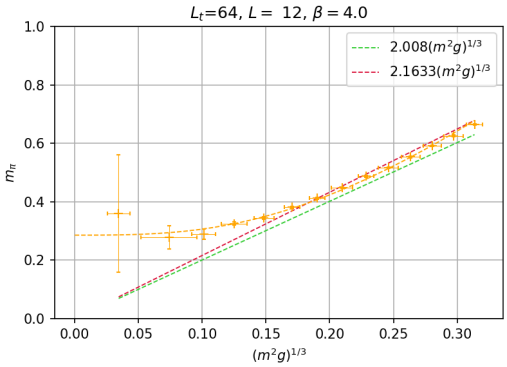

(f) m_π vs. $(m^2g)^{1/3}$ for $L = 12$. m_π =0.2857(41)

Figure 4.4: Results for $\beta = 4$. Each value was obtained by averaging 1,000 measurements of different configurations. Between each configuration used, 10 sweeps were performed.

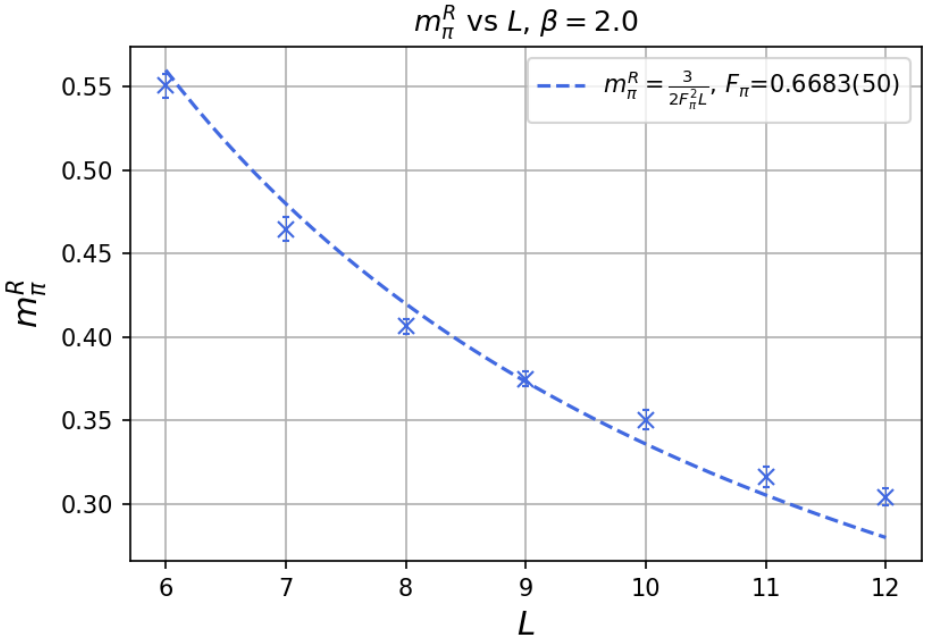

Figure 4.5: m_π^R vs. L for $\beta = 2$.

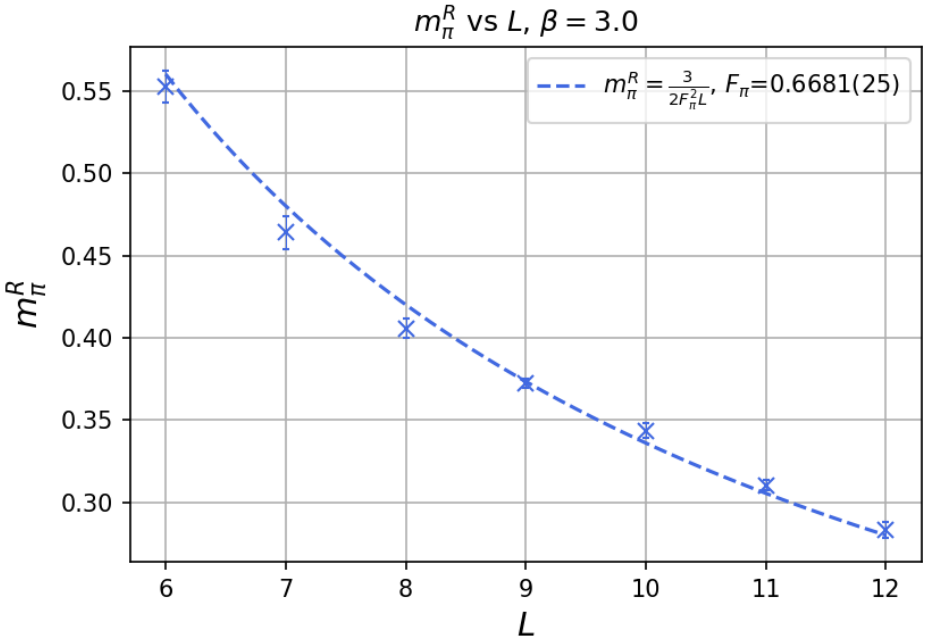

Figure 4.6: m_π^R vs. L for $\beta = 3$.

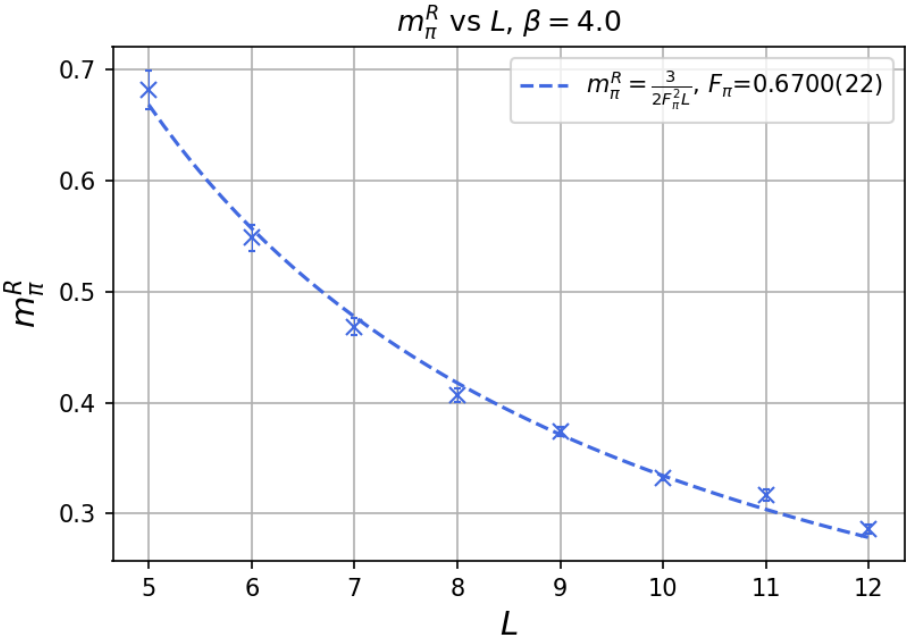

Figure 4.7: Behavior of m_π^R vs. L for $\beta = 4$. We can see that it matches the behavior of $1/L$ described in eq. (4.28). When L becomes large the residual pion mass vanishes, as it should do for an infinite volume.

The results obtained for the pion decay constant are shown in table 4.1.

β	2	3	4
F_π	0.6683(50)	0.6681(25)	0.6700(22)

Table 4.1: Pion decay constant for different values of β.

Some quantities regarding the algorithm, like the topological charge Q (figures 4.8, 4.9 and 4.10) and the autocorrelation time τ (figures 4.11, 4.12 and 4.13) were measured as well.

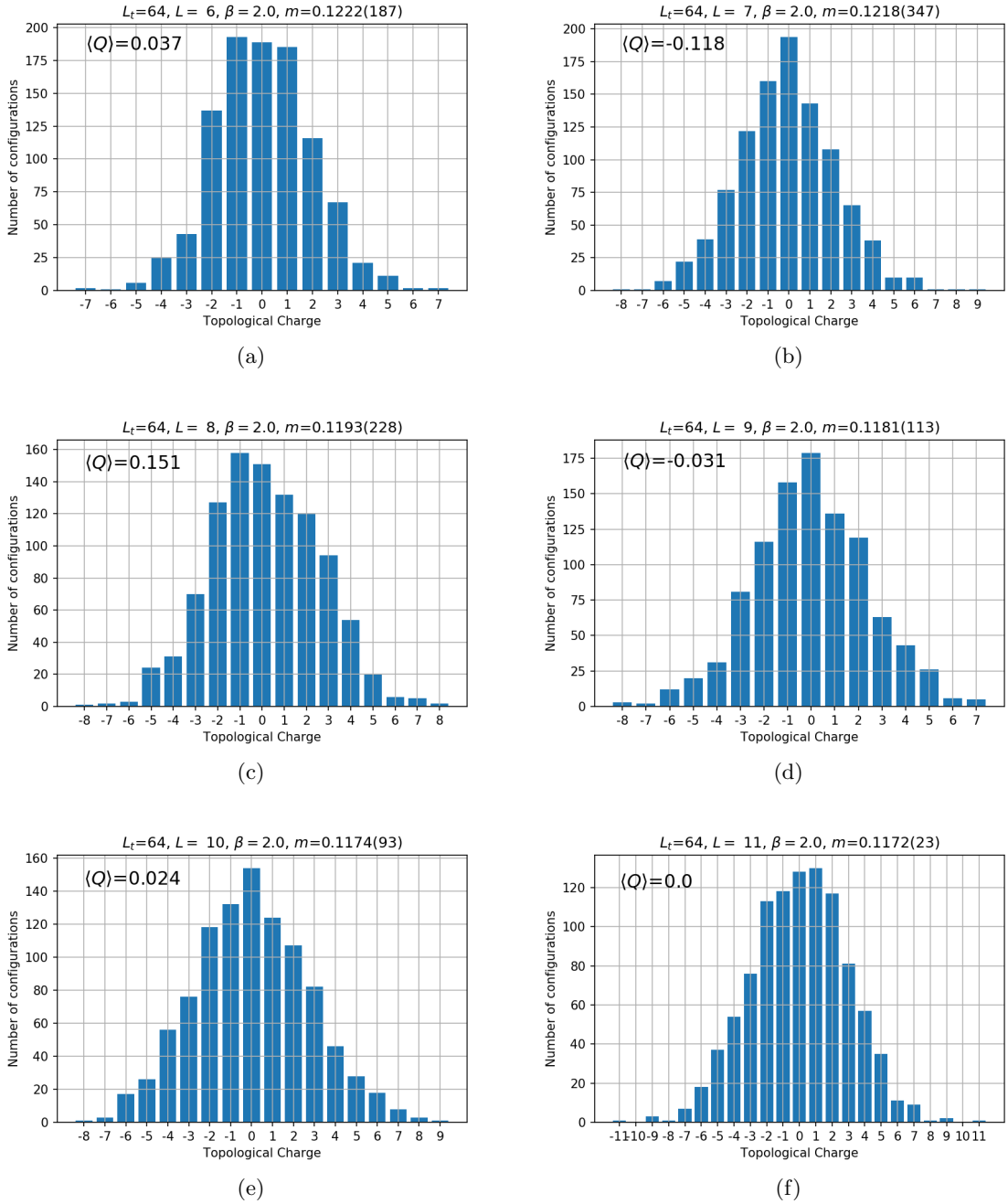

Figure 4.8: Topological charge distribution for the different lattices and fermion mass, $\beta = 2$.

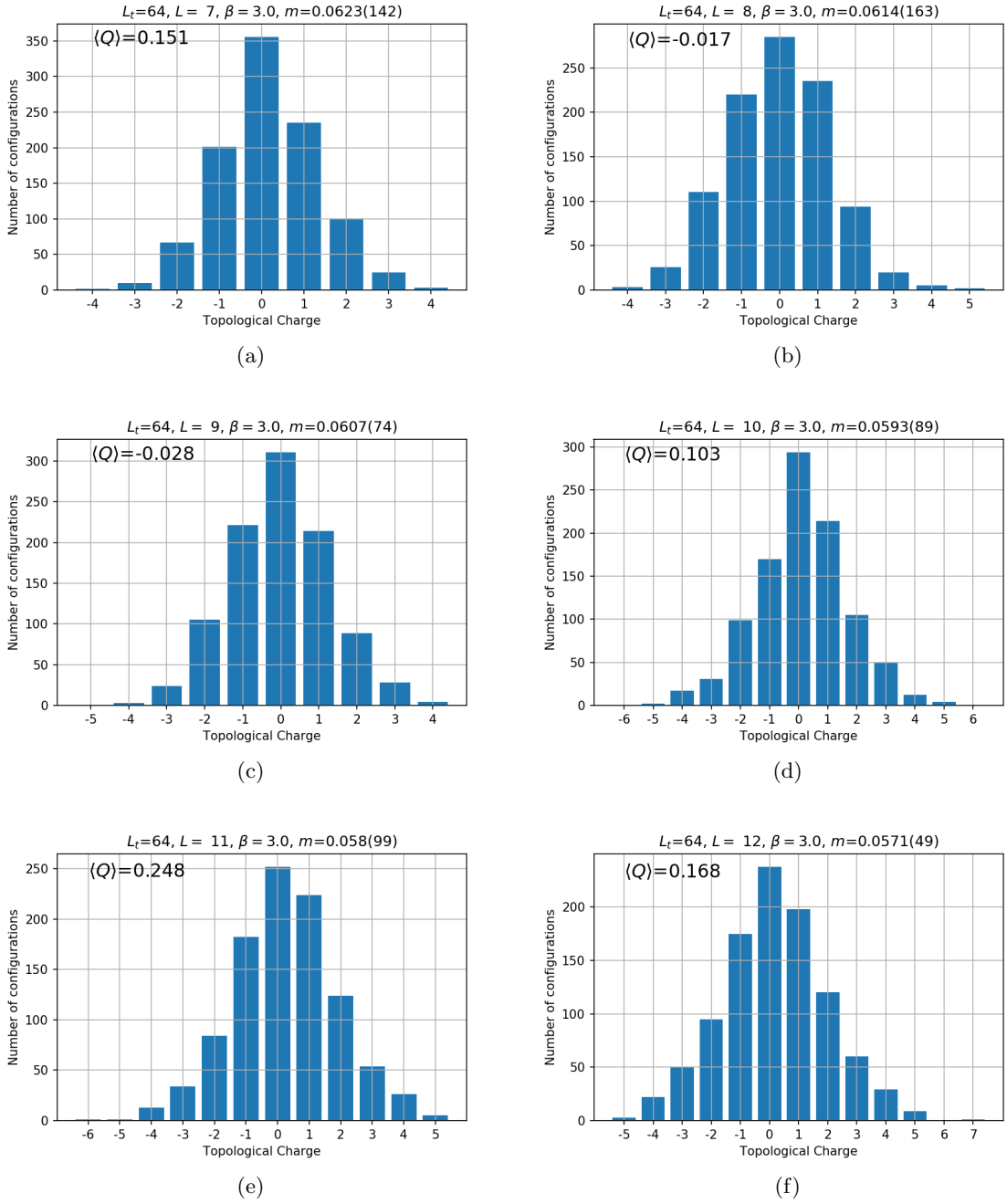

Figure 4.9: Topological charge distribution for the different lattices and fermion mass, $\beta = 3$.

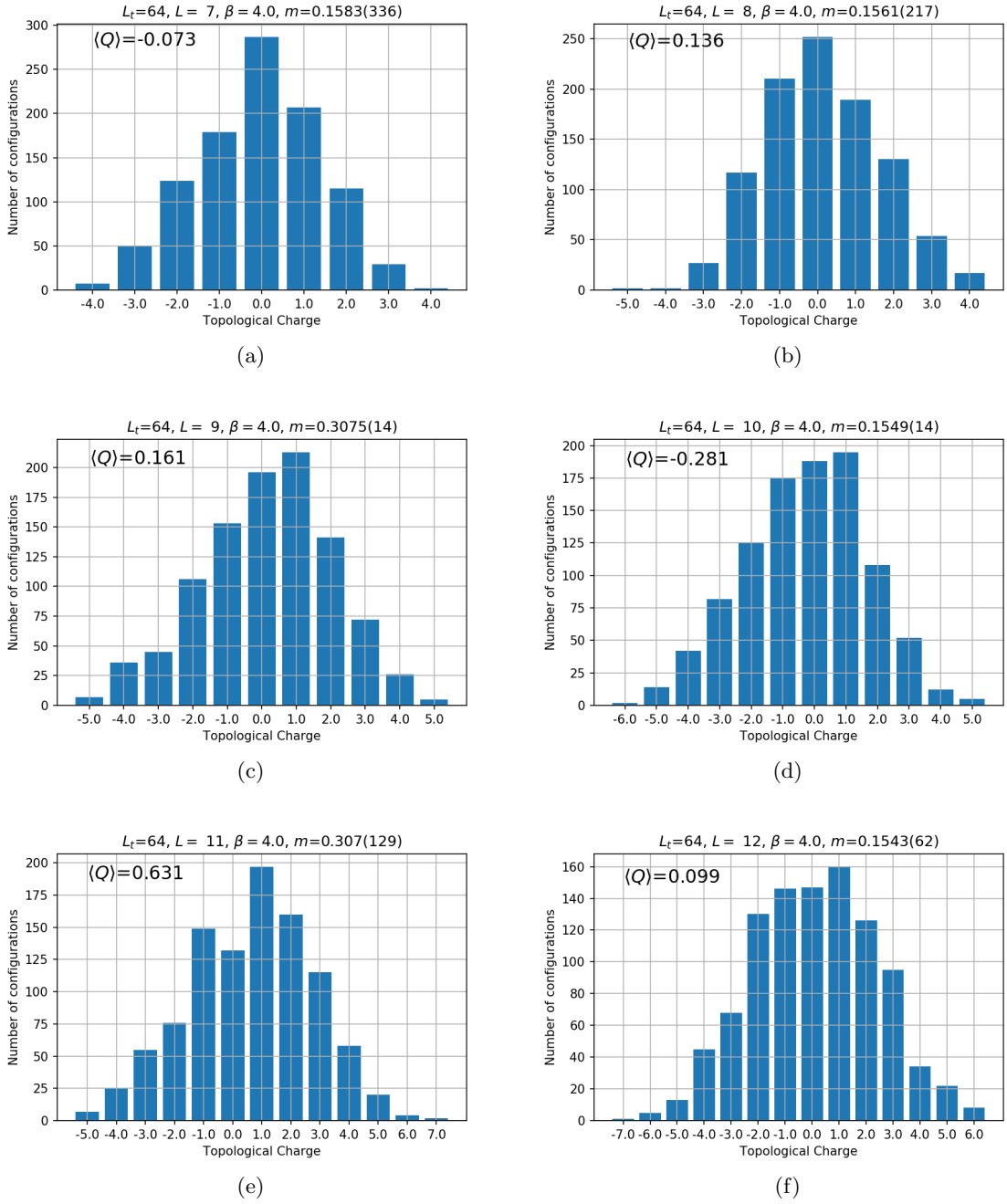

Figure 4.10: Topological charge distribution for the different lattices and fermion mass, $\beta = 4$.

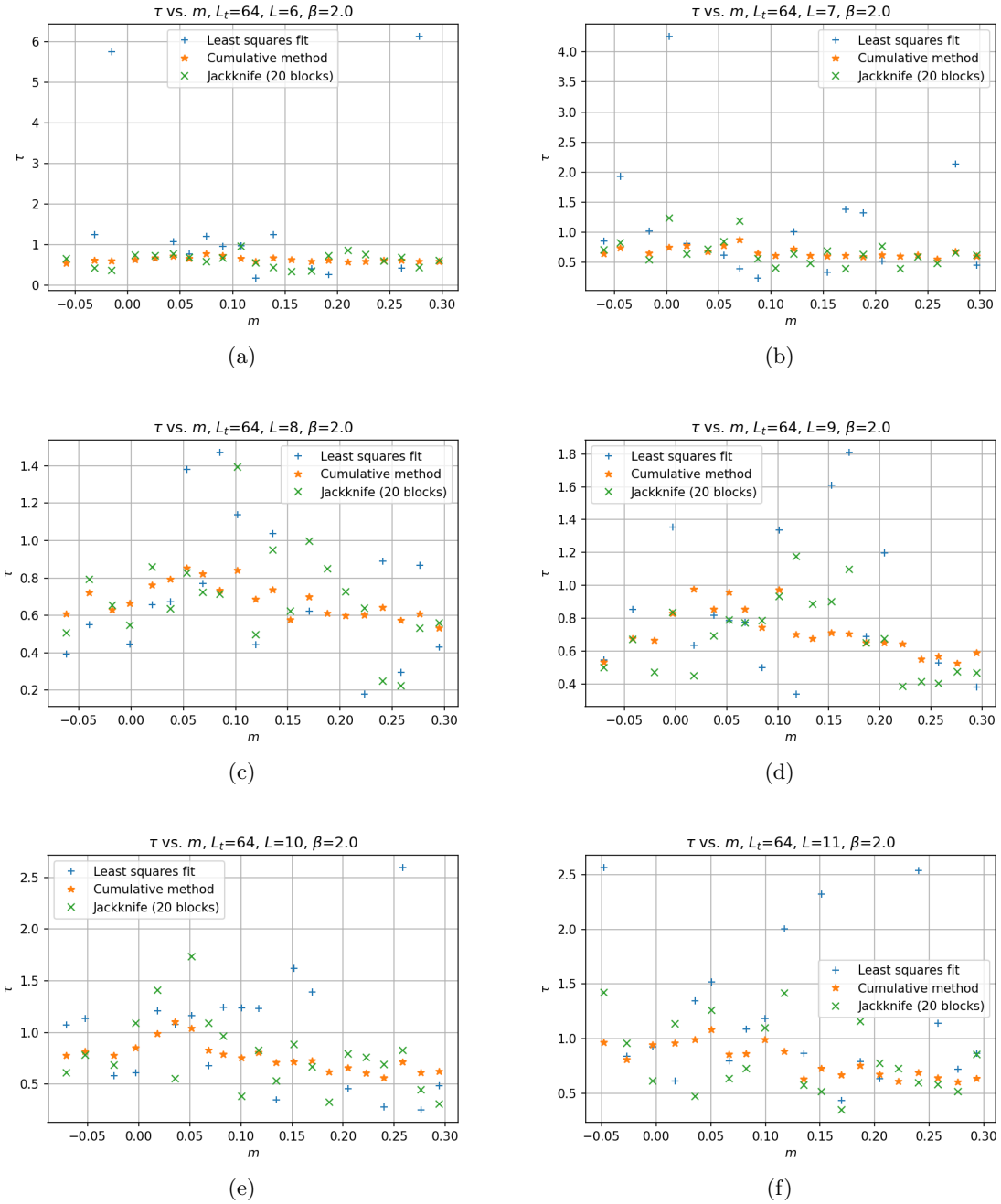

Figure 4.11: Autocorrelation time τ for different lattices, $\beta = 2$.

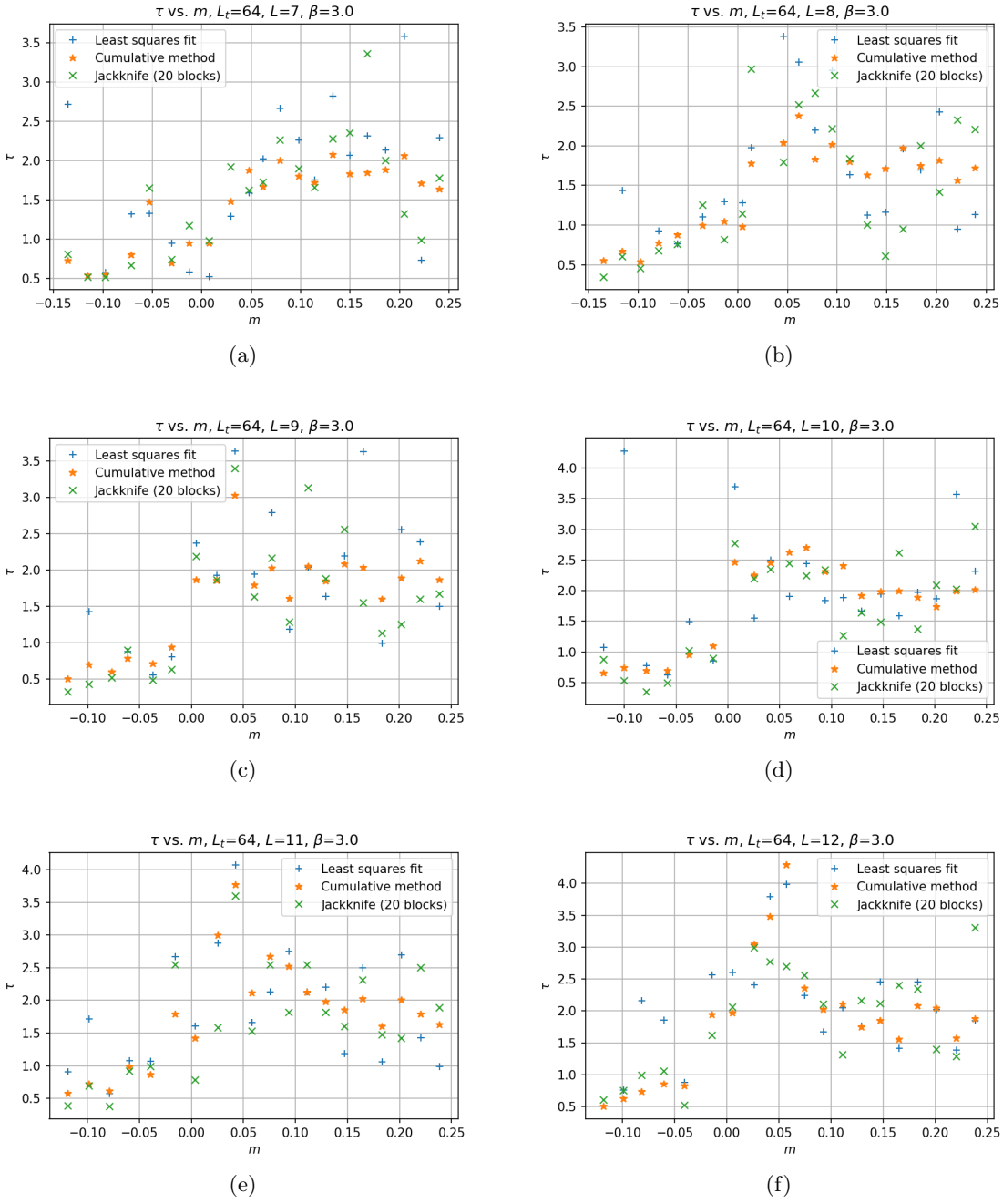

(a) (b) (c) (d) (e) (f)

Figure 4.12: Autocorrelation time τ of the topological charge for different lattices, $\beta = 3$.

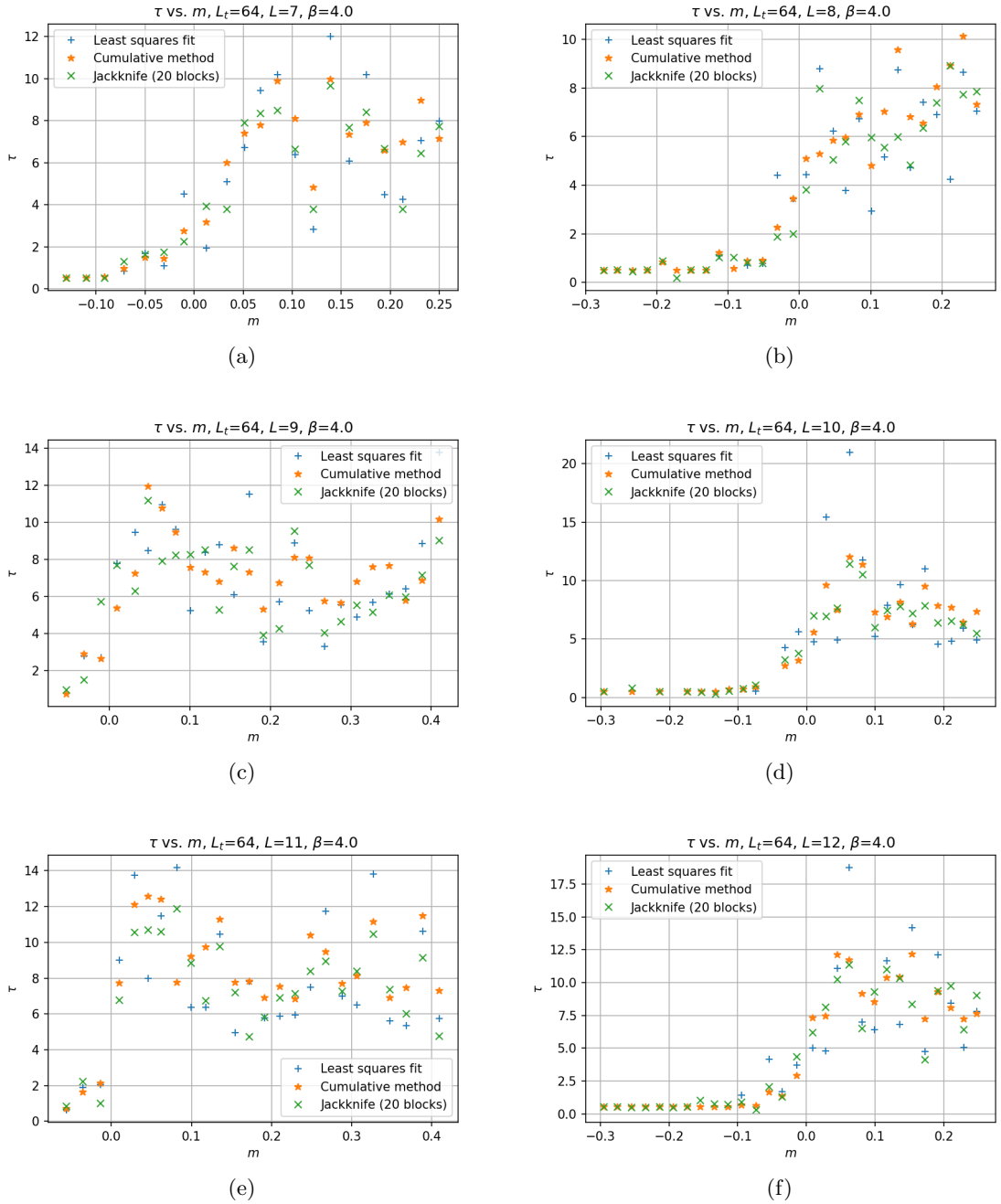

Figure 4.13: Autocorrelation time τ of the topological charge for different lattices, $\beta = 4$.

Bibliography

[1] P.A. Zyla et al. Review of Particle Physics. *Prog. Theor. Exp. Phys.*, 2020(8):083C01, 2020.

[2] S. Scherer and M. R. Schindler. *A Primer for Chiral Perturbation Theory*. Springer, 2012.

[3] A. Pich. Chiral perturbation theory. *Rept. Prog. Phys.*, 58:563–610, 1995.

[4] H. Leutwyler. Chiral perturbation theory. *Scholarpedia*, 7(10):8708, 2012.

[5] J. Gasser and H. Leutwyler. Light Quarks at Low Temperatures. *Phys. Lett. B*, 184:83–88, 1987.

[6] P. Hasenfratz and H. Leutwyler. Goldstone Boson Related Finite Size Effects in Field Theory and Critical Phenomena With O(N) Symmetry. *Nucl. Phys. B*, 343:241–284, 1990.

[7] J. Gasser and H. Leutwyler. Thermodynamics of chiral symmetry. *Phy. Lett. B*, 188(4):477–481, 1987.

[8] M. Golterman. Applications of Chiral perturbation theory to lattice QCD. In *Les Houches Summer School: Session 93: Modern perspectives in lattice QCD: Quantum field theory and high performance computing*, pages 423–515, 12 2009.

[9] S. Aoki et al. Review of lattice results concerning low-energy particle physics. *Eur. Phys. J. C*, 77(2):112, 2017.

[10] A. Bazavov et al. Results for light pseudoscalar mesons. *PoS*, LATTICE2010:074, 2010.

[11] R. Arthur, T. Blum, P. A. Boyle, N. H. Christ, N. Garron, R. J. Hudspith, T. Izubuchi, C. Jung, C. Kelly, A. T. Lytle, R. D. Mawhinney, D. Murphy, S. Ohta, C. T. Sachrajda, A. Soni, J. Yu, and J. M. Zanotti. Domain wall QCD with near-physical pions. *Phys. Rev. D*, 87:094514, May 2013.

[12] E. Follana, C. T. H. Davies, G. P. Lepage, and J. Shigemitsu. High-Precision Determination of the π, K, D, and D_s Decay Constants from Lattice QCD. *Phys. Rev. Lett.*, 100:062002, Feb 2008.

[13] W. Bietenholz, M. Göckeler, R. Horsley, Y. Nakamura, D. Pleiter, P.E.L. Rakow, G. Schierholz, and J.M. Zanotti. Pion in a box. *Phy. Lett. B*, 687(4):410–414, 2010.

[14] H. Leutwyler. Energy Levels of Light Quarks Confined to a Box. *Phys. Lett. B*, 189:197–202, 1987.

[15] P. Hasenfratz and F. Niedermayer. Finite size and temperature effects in the AF Heisenberg model. *Z. Phys. B*, 92:91, 1993.

[16] S. R. Coleman. There are no Goldstone bosons in two-dimensions. *Commun. Math.*

Phys., 31:259–264, 1973.